Self-Powered Wireless Nano-scale Sensor Networks within Chemical Reactors

Eisa Zarepour[1] Mahbub Hassan[1] Chun Tung Chou[1]
Adesoji A. Adesina [2]

[1] School of Computer Science and Engineering
University of New South Wales, Australia
{ezarepour, mahbub, ctchou} @cse.unsw.edu.au

[2] ATODATECH LLC, Brentwood, CA 94513 USA
ceo@atodatech.com

Technical Report
UNSW-CSE-TR-201423
October 2014

THE UNIVERSITY OF
NEW SOUTH WALES

School of Computer Science and Engineering
The University of New South Wales
Sydney 2052, Australia

Abstract

Because of their small size and unique nanomaterial properties, nano-scale sensor networks (*NSNs*) can be applied in many chemical applications to monitor and control the chemical process at molecule level. Nano-sensors can take advantage of the temperature variation during a chemical synthesis to harvest thermoelectric energy from each individual reaction. In this study, we demonstrate that how the *thermal property* of chemical reactions could be used as a practical source for energy harvesting for the nanosensor nodes deployed in the catalyst sites to form a self-powered NSNs.

1 Introduction

Wireless nano-scale sensor networks (*NSNs*) [3] can be potentially used to monitor and control physical, chemical and biological processes. In our earlier work [21, 23, 20], we have shown how a NSN could be deployed inside a reactor for a bottom-up control of the chemical synthesis with the ultimate goal of improving the performance of the reactor.
In addition, due to the size and energy constraints of nanosensors and also high molecular absorption noise and attenuation in the terahertz channel, the working frequency of the nano-antennas, designing simple, reliable and energy efficient communication protocols is one of the active ongoing research area in *NSNs* [2, 6, 24, 22]. In [22, 24], in order to provide high reliable communication in composition varying NSNs, we have proposed two novel energy efficient communication protocols respectively, by adjusting the transmission power and changing the operating frequency when the composition of the medium changes. In all our previous works, we have considered a battery-powered NSNs i.e. each nanomotes has a continues power supply from a nano-battery. In this work, we explore the possibility of running a self-powered NSN within a chemical reactor i.e. nanomotes harness power from the chemical environment.
The rest of the report is organised as follows. We overview NSNs for chemical reactors in Section 2. In the Section 3, a self-powered NSNs using thermoelectric nano-scale energy harvesting interfaces will be introduced following by the numerical results in Section 4. We conclude the report in Section 5.

2 NSN for Chemical Reactors

Catalysts are often used in chemical reactors to speed up the reaction process. The surface of a catalyst contains numerous *sites* where reactants (molecules) adsorb and react with each other. Only one molecule can be adsorbed in an empty site at any given time and it can only react with a molecule adsorbed in another close-by site. After a reaction between two molecules in two close-by sites, a different molecule is formed in either of the two sites, making one of them empty again. This process continues until all input molecules are used up. Some composite molecules desorb from the sites, which become the (desired or unwanted) output of the reactor. A nano-sensor can be deployed at each site as part of catalyst preparation. Then by forming a NSN between nanomotes in the surface of catalyst, NSNs would be able to monitor and control chemical reactions at the molecular level [21, 23, 20].
For example, figure 2.1 shows a magnified view of a catalyst and a proposed NSN with nanomotes filling up each site. Such NSN which each nanomote assumed to be capable of sensing the molecule type adsorbed (or attempting to adsorb) in the site, communicate with other nanomotes in the vicinity, and perform actuation to prevent adsorption of specific molecule types, can potentially control the whole synthesis and finally improve the performance of the reactor i.e. increasing the ratio of the desired product in the output [20]. Each nanomote is powered by either a limited-capacity nano-batteries [13, 14] or a limited-throughput energy-harvesting circuits [12, 15]. However, due to size limitation and extremely large number of the nanomotes in the surface of the catalyst (1 trillions site per m^2), battery-powered NSNs might not be a feasible

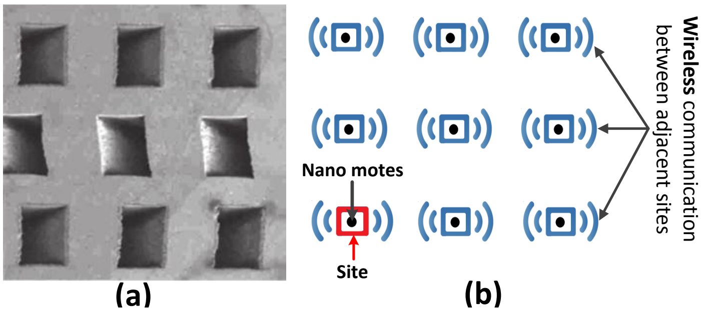

Figure 2.1: (a) A scanning electron microscopy image (adapted from [10]) showing that the sites are arranged in a regular 2D grid, (b) an imaginary 3x3 nano sensor grid where each site hosts a nanomote.

approach for chemical catalysis. In contrast, there are few options to harvest energy during a chemical synthesis to power a NSNs that is operating within a chemical reactor. First, as the pressure of the reactor is variable over time, due to production and consumption of species, the piezoelectric nano-generator [16] that is able to convert pressure variation to electricity, can be used to feed a self-powered NSNs. Second, wireless radiation from nano-motes is also another opportunity to scavenge power using a RF power generator [11]. Finally, due to endothermic and exothermic behaviour of reactions, the instantaneous temperature variation during the synthesis can potentially be utilized to harvest thermoelectric power [18].

In this work, we study energy harvesting from temperature variation and leave the rest of potential options as a future works. For that, we use a nano-scale Pyroelectric Energy Harvesting device (Pyro-EH) [18] which is able to convert any temperature variation to the electricity. In order to make the discussion concrete, we chosen Fischer-Tropsch (FT) synthesis which is a major process for converting natural gas to liquid hydrocarbons in a batch chemical reactor [1]. We will briefly overview FT synthesis in the next section.

2.1 Fischer-Tropsch Reactor

FT synthesis is a major process for converting gas (either natural gas or synthesis gas from gasification of coal) to liquid hydrocarbons. The reactor starts with a specific amount of carbon monoxide CO and hydrogen H_2. Many chemical species are produced and consumed, via many different chemical reactions, during the synthesis. The synthesis stops when no more new products are produced. The contents of the reactor is then emptied to enable the next round of synthesis to begin. The overall function of FT synthesis can be depicted as the black-box of figure 2.2 but it contains 10 main elementary steps including two absorption phases and 8 categories of reactions which has been listed in the Table 2.1. The main outputs of the FT process are olefins (desired), paraffin (undesired) and water.

Chemical reactions can be exothermic, i.e., they produce heat in the site when the reaction takes place, or endothermic, i.e., they consume heat from the

Table 2.1: Released Energy in KJ/mol for Fischer-Tropsch Elementary Reactions

	Reaction	Released Energy (KJ/mole)
Adsorption Phase		
R_1	$CO + 2s \longrightarrow C_{(s)} + O_{(s)}$	56.5
R_2	$H_2 + 2s \longrightarrow 2H_{(s)}$	10.4
Water Formation		
R_3	$O_{(s)} + H_{(s)} \longrightarrow OH_{(s)} + s$	103.80
R_4	$OH_{(s)} + H_{(s)} \longrightarrow H_2O_{(s)} + s$	86.22
Chain Initiation		
R_5	$C_{(s)} + H_{(s)} \longrightarrow CH_{(s)} + s$	77.66
R_6	$CH_{(s)} + H_{(s)} \longrightarrow CH_{2(s)} + s$	11.94
R_7	$CH_{2(s)} + H_{(s)} \longrightarrow CH_{3(s)} + s$	61.88
Chain Growth		
R_8	$C_nH_{2n+1(s)} + CH_{2(s)} \longrightarrow C_mH_{2m+1(s)}$ (m=n+1)	44.79
Hydrogenation to Paraffin		
R_9	$C_nH_{2n+1(s)} + H_{(s)} \longrightarrow C_nH_{2n+2} + 2s$	117.75
β -Dehydrogenation to Olefin		
R_{10}	$C_nH_{2n+1(s)} \longrightarrow C_nH_{2n} + H_{(s)}$	96.27

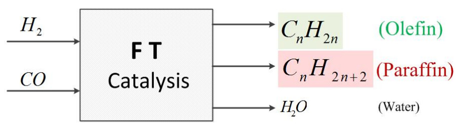

Figure 2.2: Input and output of Fischer-Tropsch Catalysis.

environment. FT synthesis is highly exothermic and the released energy comes from its elementary reaction steps. The last column of table 2.1 shows the amount of released energy per mole [8] for each category of reactions. The heat changes create a temperature gradient which can be harvested by pyroelectric generators [18]. The harvested energy can be stored in a capacitor to power each nanomotes resigning in a site. In the next section, we demonstrate that how the *thermal property* of chemical reactions could be used as a practical source for energy harvesting for the nanosensor nodes deployed in the catalyst sites.

3 Pyro-EH self-powered NSNs

The pyroelectric nano-generator converts any temperature variation to electricity using the following principles. The detectable current $i(t)$ of a pyroelectric material is proportional to the rate of change of its temperature and can be expressed as [18]:

$$i(t) = P_C \times A \times (\frac{dT(t)}{dt}) \quad (3.1)$$

where P_C is the pyroelectric current coefficient of the material, which is measured experimentally by measuring the output current [7]. A is the surface area of the electrode connected to the pyroelectric material during measurements. The larger electrode will collect larger number of electrons and hence the measured current will increase. Here, we assume A is equal to the size of the catalyst's site which is $2.5 \times 10^{-13} m^2 (0.5\mu m * 0.5\mu m)$. The dT/dt denotes the temporal temperature gradient. Larger changes in temperature in shorter periods of time generate larger output current. Pyroelectric current coefficient depends on the material of the nanogenerator. The second column of the Table 3.1 shows the experimental value of P_C for few different materials [7]. In this work, we use the proposed ZnO pyroelectric nanogenerator in [18] which has a coefficient of 15 $\mu C/m^2K$.

Table 3.1: Pyroelectric current and voltage coefficient of various materials

	Material	$\|P_C\|$ **(units** $\mu C/m^2K$**)** **[7]**	P_V **(units** V/m^2K**)** [9]
1	Triglycine sulfate TGS	270	1200
2	LiTaO3	176	650
3	BaTiO3	200	105
4	$PbZr_{0.95}Ti_{0.05}O_3$	268	500
5	ZnO	9.4 to 15	$2.5 - 4 \times 10^4$

Similarly, pyroelectric voltage at time t can be calculated as:

$$V(t) = P_V \times r_d \times \Delta T(t) \quad (3.2)$$

where P_V is pyroelectric voltage coefficient, r_d is the Debye length of ZnO (about 50 nm) and $\Delta T(t)$ is the variation of temperature at time interval of $[t-1, t]$ in Kelvin. The last column of Table 3.1 shows pyroelectric voltage coefficient for 5 different materials. The harvested power is simply the product of $i(t)$ and $V(t)$.

Production (or consumption) of heat by the reactions would increase (or decrease) the temperature of the site. This instantaneous temperature variation could be converted to electrical energy by a pyroelectric energy harvester fitted to the nanosensor node. In the next section, the methodology of extracting the temperature variation and the rate of variation in each single site via each reaction, respectively ΔT_{R_s} and $(dT/dt)_{R_S}$ will be described.

3.1 Heat Analysis of FT syntheis

The last column of Table 2.1 illustrates the amount of released heat during each individual reaction per mole, Q_R. However, in order to calculate the harvestable power via pyroelectric nanogenerator [18] for each single nanomote residing in a site, the variation in the temperature and the rate of variation both via each reaction in each site, (ΔT_R) and $(dT/dt)_R$, respectively, is required. In the next section, we derive these two parameter from Q_R and catalysts specification.

Catalyst and Site Specifications

We assume an iron-based fixed-bed FT catalyst which has been equipped with 1 trillions (10^{12}) sites per square meter (m^2) and each site has a dimension of $0.5\mu m$ by $0.5\ \mu m$. The thickness of catalyst can be varied from few nm [25] to few mm [4]. Here me assume a catalyst with 2nm thickness. As a result, each site has a volume of 5×10^{-22}. This much iron has a mass of 4fg ($m_S = 4 \times 10^{-15}$).

Variation of temperature via each reaction

The given Q_R in Table 2.1 is for consumption of one mole of each molecules during each reaction that is not valid for each site which is hosting only one single molecules.
As each mole of gas contains $K = 6.02 \times 10^{23}$ molecules, the Avogadro number and each reaction averagely consumes two moles reactants, we can translate the total released heat to the released energy per site, Q_{R_s} as:

$$Q_{R_s} = \frac{2 \times Q_R}{K} \tag{3.3}$$

The relationship between quantity of released energy via reaction R in site S, S, Q_{R_s} , and site temperature rise when the reaction occurs is :

$$\Delta T_{R_s} = \frac{Q_{R_s}}{m_S \times C_p} \tag{3.4}$$

where C_p is the specific thermal capacity of the surface in $J^{-1}gK^{-1}$ (0.45 for iron), m_S is the mass of surface involved in each site in g and ΔT_{R_S} is the temperature change during the reaction R within site S in Kelvin. Figure 3.1 shows the temperature variation in each site during different reactions.

The rate of change in temperature via each reaction

In order to calculate the rate of temperature change (K/s), we need to have an estimation for reaction time that is the source of variation in the heat. *Volumetric flow rate*,V_f , or the *superficial velocity*, S_V, could be used to find the approximation of reaction time. For example, S_V shows how much syngas (in m^3) is consumed per surface area (m^2) per time (second) [17].
The *superficial velocity* for an FT reactor is a design variable informed by several considerations such as minimisation of transport effects, pressure drop, etc. In this study we use $S_V = 0.25\, ms^{-1}$ [19] which means 0.12 cubic meter of feeding gas will be consumed in one second in 1 square meter of the catalyst.

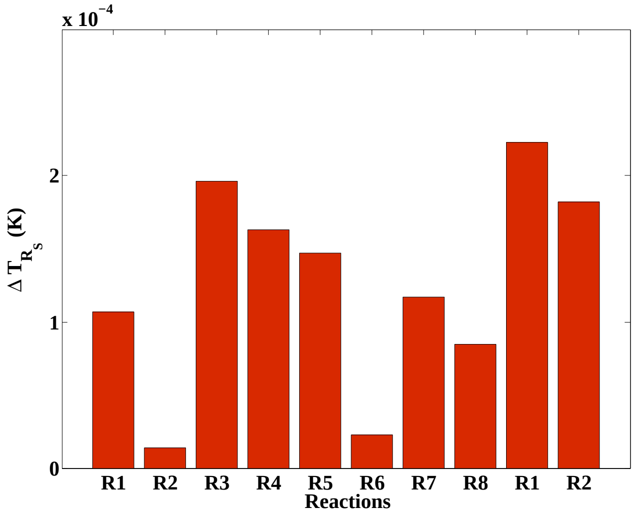

Figure 3.1: Variation of temperature during each reaction in each individual site

As all reactions needs 2 molecules to initiate the reactions (except R_8 that needs one), the average total number of reaction that happens in one second and one unit of catalyst surface area, $\bar{N}_R$, can be calculated as:

$$\bar{N}_R = \frac{S_V \times N_M}{2} \tag{3.5}$$

where N_M is number of gaseous molecules per cubic meter. Based on ideal gas law, N_M is:

$$N_M = \frac{PV}{K_B T} \tag{3.6}$$

where P is pressure in Pascal, T is temperature in Kelvin, V is volume of the gas in m^3 which 1 here and K_B is the Boltzmann constant that is $1.38 \times 10^{-23} m^2 kg s^{-2} K^{-1}$. From the equation 3.6, N_m is 1.4×10^{26} for temperature of 500K and pressure of 10atm . Therefore, number of reactions happening in one second on each site, $\bar{N}_{R_S}$, would be:

$$\bar{N}_{R_S} = \frac{\bar{N}_R}{S} \tag{3.7}$$

which S is number of sites per m^2 that is 10^{12}. Therefore the $\bar{N}_{R_S} = 2.72 \times 10^{12}$ and average reaction time would be 3.71×10^{-13}. For time being, we assume all reaction has the same time and speed. Figure 3.2 represents the rate of variation in the temperature in each site via each individual reaction.

4 Results

The aim of this section is to study the quantity of harvestable power during FT synthesis using the pyroelectric model that has been discussed in Section3.

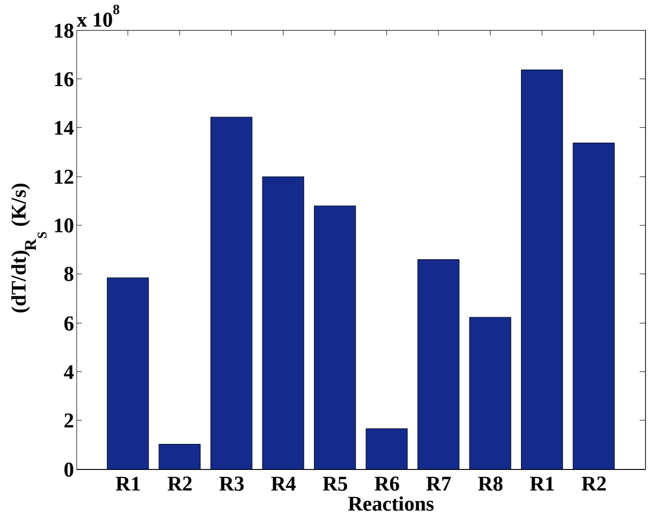

Figure 3.2: The rate of temperature variation via different reactions

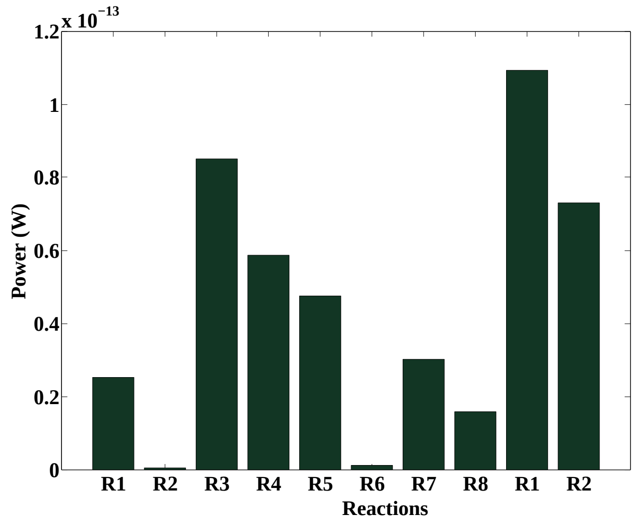

Figure 4.1: Estimating harvested power from temperature rise in a site. A site has a mass of 4 fg and thermal capacity of 0.45 J/gK. Each reaction assumed to last for a few pico seconds.

We assume equal kinetic constants of 7 for all possible reactions except water formation reactions that has been considered as 0.2. The chemical production continues until no more new chemicals can be produced. Working pressure and temperature of the reactor is considered as 10 atm and 500 K, respectively. First we present the amount of harvestable power via each category of reactions. Figure 4.1 shows the resulting harvested power due to temperature rise in each site of an iron-based FT catalyst using a Pyro-EH. The average harvestable power via this 10 reactions is 43fW $(43 \times 10^{-}15)$.

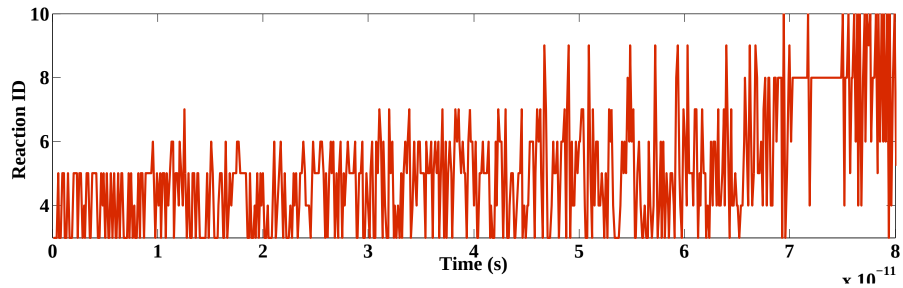

(a) The chain of the reactions.

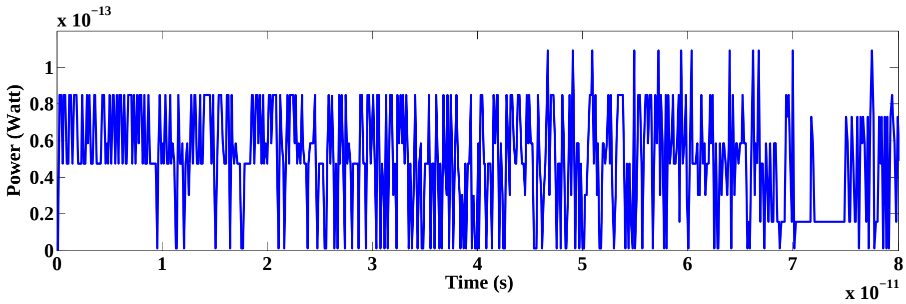

(b) Instantaneous harvested power.

Figure 4.2: Occurring reactions and resulting harvested power during FT synthesis with initial CO=200 molecules and H=500 atoms

Now we turn to study the instantaneous harvested power during FT synthesis. Using the Stochastic Simulation Algorithm (*SSA*) [5], which is a standard algorithm to simulate chemical processes, we extract the evolution of reactions over time for an FT reactor with initial input of 200 carbon monoxide molecules and 500 hydrogen atoms. Figure4.2a represents the chain of reactions including 599 reactions from 10 different categories. Using the pyroelectric model of section 3, the resulting powers have been depicted in the Figure 4.2b. The average harvestable power during this run of the FT synthesis is 49fW.

5 Conclusion

Temperature variation during a chemical synthesis due to occurrence of different reactions can be practically used to feed a self-powered nano-scale sensor network (NSNs) by using a pyroelectric nanogenerator.

Bibliography

[1] A. Adesina. Hydrocarbon synthesis via Fischer-Tropsch reaction: travails and triumphs. *Applied Catalysis A: General*, 138(2):345–367, May 1996.

[2] A. Afsharinejad, A. Davy, B. Jennings, and S. Balasubramaniam. GA-based frequency selection strategies for graphene-based nano-communication networks. *2014 IEEE ICC*, pages 3642–3647, June 2014.

[3] I. F. Akyildiz and J. M. Jornet. Electromagnetic wireless nanosensor networks. *Nano Communication Networks*, 1(1):3–19, 2010.

[4] J. P. Collins, J. J. Font Freide, and B. Nay. A History of Fischer-Tropsch Wax Upgrading at BPfrom Catalyst Screening Studies to Full Scale Demonstration in Alaska. *Journal of Natural Gas Chemistry*, 15(1):1–10, Mar. 2006.

[5] D. Gillespie. Exact stochastic simulation of coupled chemical reactions. *The journal of physical chemistry*, 81(25):2340–2361, 1977.

[6] I. T. Javed and I. H. Naqvi. Frequency band selection and channel modeling for WNSN applications using simplenano. In *Proceeding of the 2013 IEEE ICC*, pages 5732–5736. Ieee, June 2013.

[7] D. Lingam, A. R. Parikh, J. Huang, A. Jain, and M. Minary-Jolandan. Nano/microscale pyroelectric energy harvesting: challenges and opportunities. *International Journal of Smart and Nano Materials*, 4(4):229–245, Dec. 2013.

[8] G. Lozano-Blanco and J. Thybaut. Single-Event Microkinetic Model for Fischer Tropsch Synthesis on Iron-Based Catalysts. *Industrial & Engineering Chemistry Research*, 47:5879–5891, 2008.

[9] T. Moustakas, S. Mohney, S. Pearton, E. S. E. Division, and E. S. H. T. M. Division. *Proceedings of the Third Symposium on III-V Nitride Materials and Processes*. Electrochemical Society: Proceedings. Electrochemical Society, Incorporated, 1999.

[10] A. Renken and L. Kiwi-Minsker. Microstructured catalytic reactors. *Advances in Catalysis*, 53(10):47–122, 2010.

[11] R. Shigeta and T. Sasaki. Ambient RF energy harvesting sensor device with capacitor-leakage-aware duty cycle control. *IEEE SENSORS JOURNAL*, (July):1–10, 2013.

[12] R. Venkatasubramanian. Energy harvesting for electronics with thermoelectric devices using nanoscale materials. In *the proceeding of IEDM 2007, IEEE Electron Devices Meeting*, pages 367–370, Washington, DC, 2007.

[13] F. Vullum and D. Teeters. Investigation of lithium battery nanoelectrode arrays and their component nanobatteries. *Journal of Power Sources*, 146(1-2):804–808, Aug. 2005.

[14] F. Vullum, D. Teeters, A. Nyten, and J. Thomas. Characterization of lithium nanobatteries and lithium battery nanoelectrode arrays that benefit from nanostructure and molecular self-assembly. *Solid State Ionics*, 177(26-32):2833–2838, Oct. 2006.

[15] Z. L. Wang. Energy harvesting for self-powered nanosystems. *Nano Research*, 1(1):1–8, July 2008.

[16] Z. L. Wang and J. Song. Piezoelectric nanogenerators based on zinc oxide nanowire arrays. *Science (New York, N.Y.)*, 312(5771):242–6, Apr. 2006.

[17] J. H. Yang, H.-J. Kim, D. H. Chun, H.-T. Lee, J.-C. Hong, H. Jung, and J.-I. Yang. Mass transfer limitations on fixed-bed reactor for FischerTropsch synthesis. *Fuel Processing Technology*, 91(3):285–289, Mar. 2010.

[18] Y. Yang, W. Guo, K. C. Pradel, G. Zhu, Y. Zhou, Y. Zhang, Y. Hu, L. Lin, and Z. L. Wang. Pyroelectric nanogenerators for harvesting thermoelectric energy. *Nano letters*, 12(6):2833–8, June 2012.

[19] Yin Jing Dayton. *Computer Simulation of a Plug Flow Reactor for Cobalt Catalyzed Fischer Tropsch Synthesis Using*. PhD thesis, UNIVERSITY OF DAYTON, 2012.

[20] E. Zarepour, A. A. Adesina, M. Hassan, and C. T. Chou. Innovative approach to improving gas-to-liquid fuel catalysis via nanosensor network modulation. *Industrial and Engineering Chemistry Research*, 53(14):5728–5736, 2014.

[21] E. Zarepour, A. A. Adesina, M. Hassan, and C. T. Chou. Nano Sensor Networks for Tailored Operation of Highly Efficient Gas-To-Liquid Fuels Catalysts. In *the proceedings of Australasian Chemical Engineering Conference, Chemeca 2013*, Brisbane, Australia, October. 2013.

[22] E. Zarepour, M. Hassan, C. T. Chou, and A. Adesina. Frequency Hopping Strategies for Improving Terahertz Sensor Network Performance over Composition Varying Channels. In *The IEEE WoWMoM 2014*, Sydney, Australia, June, 2014.

[23] E. Zarepour, M. Hassan, C. T. Chou, and A. A. Adesina. Nano-scale Sensor Networks for Chemical Catalysis. In *the proceedings of the 13th IEEE International Conference on Nanotechnology*, Beijing, China, 2013.

[24] E. Zarepour, M. Hassan, C. T. Chou, and A. A. Adesina. Power Optimization in Nano Sensor Networks for Chemical Reactors. In *the proceedings of ACM International Conference on Nanoscale Computing and Communication*, Atlanta, Georgia, USA, 2014.

[25] B. Zeng, B. Hou, L. Jia, J. Wang, C. Chen, D. Li, and Y. Sun. The intrinsic effects of shell thickness on the FischerTropsch synthesis over coreshell structured catalysts. *Catalysis Science & Technology*, 3(12):3250, 2013.